NATIONAL RESEARCH CENTRE
«KURCHATOV INSTITUTE»
Institute for High Energy Physics
of the National Research Centre
«Kurchatov Institute»

Preprint 2019-6

A.G. Afonin, M.Yu. Bogolyubsky, A.A. Volkov, D.K. Elumakhov,
V.N. Zapolsky, A.A. Ivanilov, A.Yu. Kalinin, A.N. Krinitsyn,
V.I. Kryshkin, N.V. Kulagin, D.I. Patalakha, K.A. Romanishin,
V.V. Skvortsov, V.V. Talov, L.K. Turchanovich, Yu.A. Chesnokov

Forward Production of Nuclear Fragments in CC Collisions at Beam Energy 20.5 GeV/nucleon

Submitted to *Nuclear Physics A*

Protvino 2019

UDK 519.25.256 M–24

Abstract

Afonin A.G. et al. Forward Production of Nuclear Fragments in CC Collisions at Beam Energy 20.5 GeV/nucleon: NRC «Kurchatov Institute» – IHEP Preprint 2019-6. – Protvino, 2019. – p. 20, figs. 8, tables 5, refs.: 39.

The inclusive differential cross sections for forward production of nuclear fragments at an angle of 0° in CC collisions at beam energy 20.5 GeV/nucleon ($\sqrt{S_{NN}}$ =6.3 GeV) are presented. Measurements have been performed at the U-70 Accelerator Complex (Protvino) using a combined spectrometer on base of the beamline (№ 22). The fragments selection was carried out by measuring of ionization in scintillation counters taking into account the data from threshold Cherenkov counters and hadron calorimeter. Fragment mass was determined through Cherenkov light emission angle measured in the spectrometer of ring imaging Cherenkov radiation. Data are given for fragments with charge $1 \le Z \le 6$, atomic number $1 \le A \le 10$ and $A/Z < 3.4$ with momenta from 20 to 210 GeV/c. The measurements are compared with Fritiof model, statistical models and theoretical parameterizations. The discovered differences between theory and experiment are discussed. Presented results correspond to the highest energy for experiments with ion beams on a fixed target for forward production of nuclear fragments with momenta beyond the elastic peak.

Аннотация

Афонин А.Г. и др. Рождение вперед ядерных фрагментов в CC столкновениях при энергии пучка 20.5 ГэВ/нуклон: Препринт НИЦ «Курчатовский институт» – ИФВЭ 2019-6. – Протвино, 2019. – 20 с., 8 рис., 5 табл., библиогр.: 39.

Представлны инклюзивные дифференциальные сечения для рождения вперед под углом 0° ядерных фрагментов в CC столкновениях при энергии пучка 20.5 ГэВ/нуклон ($\sqrt{S_{NN}}$=6.3 ГэВ). Измерения выполнены на ускорительном комплексе У-70 (Протвино). Использовался комбинированный спектрометр на основе канала частиц высоких энергий (№ 22). Отбор вторичных фрагментов осуществлялся по измерениям ионизации в сцинтилляционных счетчиках с учетом данных пороговых черенковских счетчиков и адронного калориметра. Масса фрагмента определялась по углу излучению Черенковского света, измеряемому в спектрометре колец Черенковского излучения. Данные приведены для фрагментов с зарядом $1 \le Z \le 6$, атомным номером $1 \le A \le 10$ и $A/Z < 3.4$ при их импульсах от 20 до 210 ГэВ/с. Измерения сравниваются с моделью Fritiof, статистическими моделями и теоретическими параметризациями. Результаты получены при максимальной энергии для экспериментов с ионными пучками на неподвижной мишени для рождения вперед ядерных фрагментов с импульсами за пределами упругого пика.

Introduction

The possibilities to work with ion beams at the U-70 Accelerator Complex (National Research Center «Kurchatov Institute» – Institute for High Energy Physics, Protvino) have been presented in talk [1] (2008). And the creation of ion beams at the U-70 [2, 3, 4] opened up opportunities for new researches in relativistic nuclear physics. The experiment to study forward production at an angle of 0° of hadrons and nuclear fragments in AA-interactions was proposed in preprint [5]. It was suggested to employ the combined spectrometer consisting of the beamline (№ 22) [6] with nuclear targets at its head and detectors of the modified FODS setup [7] at the end to detect the produced secondary particles. Beamline rigidity was varied in the interval 6-70 GeV/c. A Monte-Carlo simulation of such employment of beamline in the experiment was performed in the framework of Geant4 [8].

The aim of this work is to study forward production of nuclei in CC collisions in the new energy range exceeding 20 GeV/nucleon, which is currently the highest value for experiments with ion beams on a fixed target for forward production of nuclear fragments with rapidities exceeding the rapidity of projectile particle. Previous data correspond to energies in the range 0.3-4 GeV/nucleon [9]-[16]. Measurements at 158 GeV/nucleon [17, 18] have been done to study forward particle production in central region.

In article [19] results of the first measurements at launching of this experiment in CA(Carbon Nucleus)-interactions at energy 25 GeV/nucleon are shown. The conference talk [20] gives the yields of light nuclei in CC(Carbon Carbon)-interactions at energy 20.5 GeV/nucleon ($\sqrt{S_{NN}}$ =6.3 GeV).

In this paper the measured Lorentz invariant inclusive differential cross sections are presented for forward production of nuclear fragments in CC collisions at beam energy 20.5 GeV/nucleon. The obtained experimental data are compared with Fritiof model (integrated in Geant4), statistical models and theoretical parametrizations.

1. Experimental setup

A schematic diagram of the setup is presented in Figure 1. The ^{12}C beam from the accelerator hit on a target installed after the magnet M1. A carbon target with 2 cm length and 3 cm diameter was used. Empty target runs were also taken with collection of data for the background subtraction.

Secondary particles were transported by the beam channel to the analyzing detectors. The corresponding values of momentum acceptance and angular acceptance were $\Delta p/p$=1.2% and $d\Omega$=3.4 μsr. The beamline rigidity (p/Z) was varied in the interval 6-70 GeV/c but with exception of the forbidden region 36-46 GeV/c for the technical reasons. This allowed the measurements of charged particles and ions production in a wide range of rapidities with an upper bound considerably exceeding the rapidity of initial beam particle.

Beam intensity (about 10^9 ^{12}C nuclei per spill with a duration of 1.2 s) was measured by the Secondary Emission Chambers (SEC) [21]. The absolute calibration of the SEC was done in special experiments with a current transformer also measuring intensity of the same beam. The current transformer was relatively easily calibrated in absolute units using a reference electric charge. At the beginning of measurement runs beam parameters and absolute beam intensity were defined by means of a radiochromic dosimetric film. The subsequent periodic control was performed with a mobile scintillation counter. In the region of target the beam had dimensions approximately 4 mm in vertical and 12 mm in horizontal axes.

The analyzing part of the setup shown in the bottom of Figure 1 was installed after the vacuum guide and consisted of a set of threshold Cherenkov counters, scintillation counters, a tracking system built of drift chambers and tubes [22], a spectrometer of ring imaging Cherenkov radiation (RICH) [23] and a hadron calorimeter [24].

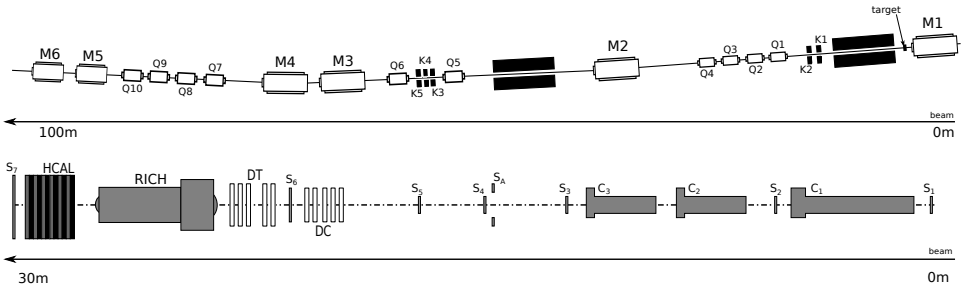

Figure 1. Schematic presentation of the experimental setup built of the beamline (№ 22) (top) and analyzing detectors of the FODS (bottom). The beam propagates from right to left. The notations are: M – magnets, Q – quadrupole lenses, K – collimators, beam dump parts are shown as solid black rectangles, S – scintillation counters, C – threshold Cherenkov counters, DC – drift chambers, DT – drift tubes, RICH – spectrometer of ring imaging Cherenkov radiation, HCAL – hadron calorimeter.

2. Experimental method

The experimental procedures were based on processing of data from the FODS detectors at known value of the beamline rigidity. In analysis the single particle events were selected according to amplitudes of the signals from scintillation counters taking into account the results of reconstruction in the tracking system. The charge of particle Z was measured from energy loss in the scintillation counters, intensity of Cherenkov light in the threshold Cherenkov counters and amplitude A_H of signal from the hadron calorimeter. The value of A_H is proportional to product $Z \cdot P_0$, where P_0 is the known beamline rigidity. Particle identification was provided by the threshold Cherenkov counters, the hadron calorimeter and the RICH. The last played the main key role. The Cherenkov light emission angle θ measured in the RICH is expressed by the formula

$$\cos(\theta) = 1/(\beta \cdot n) \tag{1}$$

through refractive index n of the medium and β which is the ratio of particle momentum P to its energy. The known values of track angle, Cherenkov emission angle, charge Z and set beamline rigidity P_0 made it possible to reconstruct the particle mass M_{reco} in the RICH from formula (1)

$$M_{reco} = P\sqrt{(n \cdot \cos(\theta))^2 - 1}\ , \tag{2}$$

where $P{=}Z \cdot P_0$.

The RICH detects photons with angles from 40 to 120 mrad relative to the detector axis, while the maximum recorded angle of Cherenkov radiation in these measurements is 93 mrad. To identify the particles that do not give a ring of Cherenkov light in the RICH, for example, antiprotons with momenta less than 10 GeV/c, the presence of a single track in an event was required with absence of the signals from threshold Cherenkov counters. The threshold Cherenkov counters were necessary also for selection of particles whose yields are comparable with the residual background contribution in the distribution of reconstructed masses in the RICH. The hadron calorimeter was used to suppress events in which the energy of particles was not consistent with the beamline rigidity.

For illustration of the method Figure 2 presents as example 2D-plot Z vs M_{reco}/M_p of the nuclear fragments yields, where Z and M_{reco} denote charge and mass of the fragment, respectively, and M_p is the proton mass. Background particles generated due to interactions on the beamline material and decays give some contribution to the shown distribution. The cross sections were determined from the mass spectrum fit taking into account the background. It was mainly located outside the physical peaks so as the momenta of background particles differ from the value required by the beamline rigidity. The observed positions of the produced nuclear fragments peaks and the background shape are reproduced by the Monte-Carlo calculations.

Crucially important in the experiment for definition of the cross sections is the calculation of setup acceptance and attenuation of the produced particle flux in the spectrometer. For this aim Geant4 (version 10.02.p02) [25] was used. The Monte-Carlo simulation of the

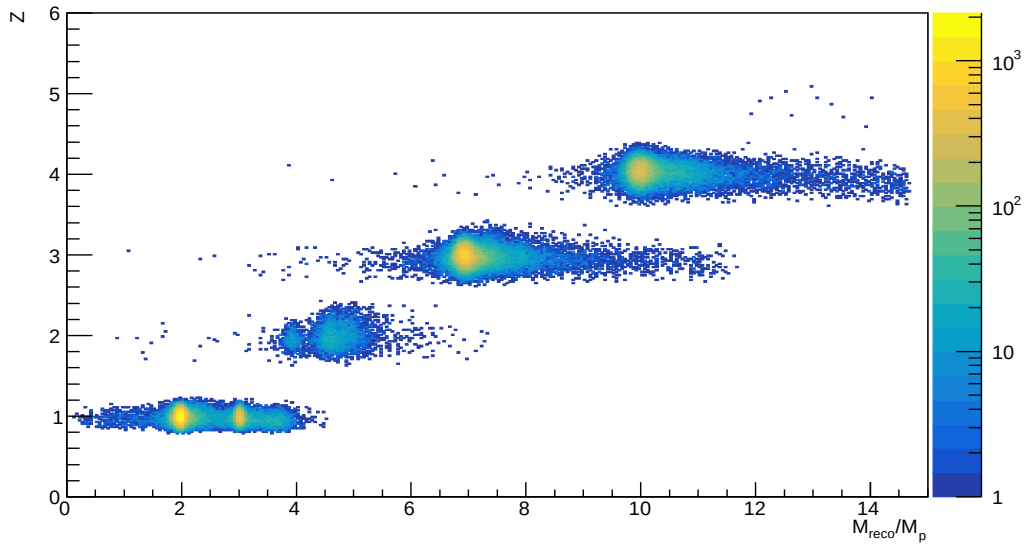

Figure 2. 2D-plot Z vs M_{reco}/M_p of the nuclear fragments yields, where Z and M_{reco} denote respectively charge of the fragment and its mass reconstructed in the RICH on the base of formula (2), M_p is the proton mass.

experiment [26] was done taking into account the experimental event selection criteria. The passage through the setup of hadrons and light nuclei proton (p), deuteron (d), tritium (t) as well as heavier various isotopes (He, Li, Be, B, C) were studied. In addition to the acceptance for each type of particles and nuclei the attenuation of the produced particle flux due to decays and interactions in the spectrometer matter was determined. The fraction of fragments eliminating from the ensemble due to these reasons varied from 28% to 77% [26] depending on the type of particles and their momentum.

The effectiveness of the accepted selection procedures for elimination of secondary particles produced in interactions in matter of the setup was taken into account. Effects of impurities from other nuclei in the ^{12}C beam as well as instability of the beam position on the target were also studied in the framework of this Monte-Carlo simulation, and they were added to systematical errors.

In the calculations the composite QGSP-FTFP-BERT-EMV model [27, 28] from Geant4 has been chosen for a transport code. It was constructed from a number of components such as the quark-gluon string model of hA-interactions (QGSP), the Fritiof AA-model (FTFP) handling the formation of initial strings and following fragmentation into hadrons according to the Lund model in the framework of Bertini (BERT) cascade, de-excitation of the remnant nucleus in the precompaund part and CPU optimization of electromagnetics (EMV). In the simulation FTFP-BERT-EMV model was used as generator of primary interactions in the target.

In the considered procedure the measured cross section was corrected to account for the target thickness. In these calculations it was used the value of total cross section σ_{tot}

for CC-interactions defined with the formula (2) from [29], based on an approximation of the experimental data in so-called geometrical model. This formula gives σ_{tot} = 850 mb, which agrees with calculations of σ_{tot} in the framework of FTFP-model.

3. Uncertainties of the experiment

The most significant uncertainty in the presented cross sections measurements arises due to the error in calibration of the beam monitor which reaches 30%.

To find the contribution of the beam instability during physical runs of the data collection to the overall uncertainty several runs were processed. The resulting error is 15% which is consistent with contribution from the beam position instability on the target simulated in the Monte-Carlo procedure.

The quality of the result is influenced by impurities of foreign nuclei in the beam. Special experiments have been performed with empty target and with beam momentum corresponding to the set rigidity to measure the composition of the beam. The measured beam composition is: ^{12}C 90%, ^{10}B 1.1%, ^{6}Li 0.9%, ^{4}He 5.3%, d 2.7%. The Monte-Carlo calculations showed that a change of the carbon content in the beam to 80% should not give an error in the cross sections of more than 5%.

The next factor that can distort the results is the admixture of particles produced in the secondary interactions in beamline material or in installed detectors. The simulation has shown that the contribution from such particles does not exceed 1%. This is due to the fact that they are rejected by energy deposited in the calorimeter and the value of mass reconstructed in the RICH.

And finally note that beamline rigidity was set with systematic error 1% and this relative shift is the same to all measured points.

4. Experimental results

4.1. Dependence of inclusive zero angle cross sections on momentum in laboratory system

Obtained results on cross section measurements are collected in Tables 1 – 5 for the nuclear fragments with charge $1 \leq Z \leq 6$. Figures 3 and 4 show the dependence of zero angle spectra p, d, t, ^{3}He, ^{4}He, ^{6}He, ^{7}Li, ^{7}Be, ^{8}Li, ^{8}B, ^{9}Li, ^{9}Be, ^{10}Be, ^{10}C on fragment laboratory momentum P_{lab} in CC collisions at energy 20.5 GeV/nucleon. The experimental results are compared with predictions of the FTFP model.

It is seen that the model qualitatively describes main features of the cross sections behavior but quantitatively there are noticeable discrepancies. The data show that the maxima of distributions are shifted towards large momenta proportionally to the fragment atomic number A. All fragments are substantially produced in the region beyond the observed peaks with momenta exceeding the value $A \cdot p_0$, where p_0 is momentum of one nucleon in the ^{12}C beam, i.e. in the kinematical forbidden region in free NN collisions. Observed gaps in the presented distributions on the right slope for protons and in the

region of maximum for symmetric fragments arise for technical reasons prohibiting to set beamline rigidity in range 36-46 GeV/c.

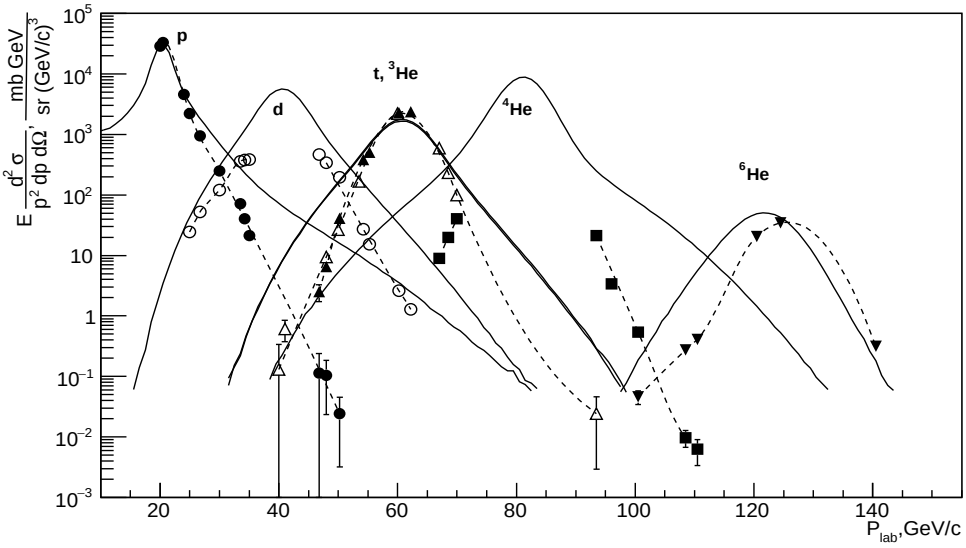

Figure 3. Lorentz invariant inclusive differential cross section versus fragment laboratory momentum P_{lab} for zero angle production of p (•), d (○), t (▲), ^3He(△), ^4He (■), ^6He (▼) in CC collisions at energy 20.5 GeV/nucleon in comparison with the predictions of FTFP model (solid lines). The dotted curves are drawn to guide the eye.

Also the comparison of dependencies presented in Figures 3 and 4 have been done with Baldin's approximation [30] which claims a universal cross section description at least at large momenta. This approximation is based on scaling invariance for nuclear processes [31] (see also [32]) with using the scaling variable introduced by V.S. Stavinskii [33] which is a minimal energy of the colliding constituents. It was found that the mentioned approach can not describe presented data on production of nuclear fragments. The discrepancy strongly grows with increase of fragment atomic number A and it reaches many orders of magnitude. Also add that a noticeable although smaller discrepancy between this experiment and Baldin's approximation exists and for forward production of charged π- , K-mesons and antiprotons. From a theoretical point of view possible mechanisms of production can be divided into two classes (see, for example, [34]): a) hot processes, where observed objects (particles, fragments) are created in an act of collision of constituents and b) cold processes, where these objects are originally present in the fragmented nucleus. These experimental results can specify that the main mechanism of forward nuclear fragments production belongs to the class of cold processes.

Introduce the variable

$$x = P_{lab}/p_0 \ , \tag{3}$$

where p_0 is the momentum of one nucleon in the incident ion beam. Figure 5 shows a comparison of the cross sections dependence on x from this experiment with analogous

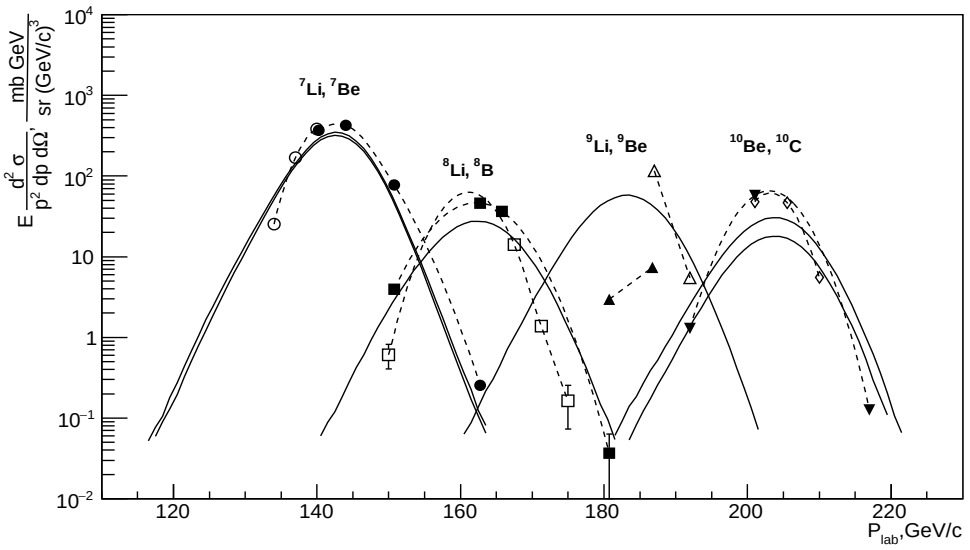

Figure 4. Same as figure 3 but for ^7Li (•), ^7Be (∘), ^8Li (■), ^8B (□), ^9Li (▲), ^9Be (△), ^{10}Be (▼), ^{10}C (◊).

measurements in forward direction in CC collisions at lower energy 1.05 GeV/nucleon [11].

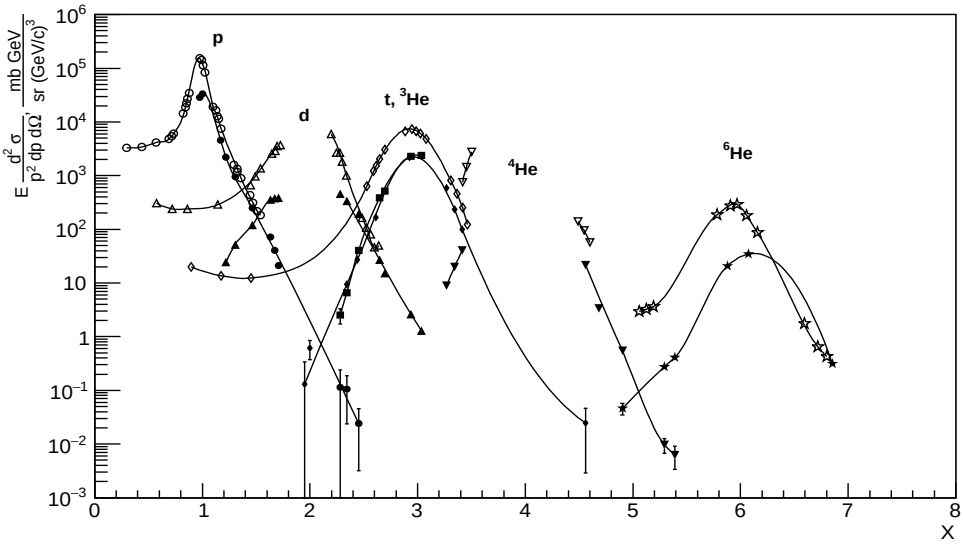

Figure 5. Comparison of the inclusive differential cross section dependence on x (see formula (3)) for zero angle production from these data (black symbols) with analogous measurements [11] in CC collisions at lower energy 1.05 GeV/nucleon (open symbols). The notations are: p (•, ∘), d (▲, △), t (■, □), ^3He (⧫, ◊), ^4He (▼, ▽), ^6He (★, ☆). The smooth curves are drawn to guide the eye.

One can see that the general dependence of cross sections on the variable x is similar, but they are noticeably lower at larger energy 20.5 GeV/nucleon than at 1.05 GeV/nucleon. The mentioned difference varied from a factor of 5 times near the fragmentation peak to several orders of magnitude beyond this peak.

The t/p ratio for the invariant differential cross sections of light nuclei from the peaks of distributions is not essential changed from $\simeq 3.5 \cdot 10^{-2}$ at energy 1.05 GeV/nucleon to $\simeq 4.5 \cdot 10^{-2}$ at 20.5 GeV/nucleon. In the STAR experiment the similar ratio $t/p \simeq 5 \cdot 10^{-4}$ was measured for integrated fragment yields for central Au-Au collisions at $\sqrt{S_{NN}}$=7.7 GeV [35]. This demonstrates a strong difference of the t/p ratio for fragmentation processes and central collisions.

At the energy of this experiment 20.5 GeV/nucleon the clear separation between projectile and target fragmentation regions is achieved. This is illustrated in the next Figure 6 where as a representative example the inclusive differential cross section versus rapidity y in laboratory system are shown for zero angle production of tritium (t) and ^3He. The data in the target fragmentation region are obtained after the reflection about the point $(y_T + y_B)/2$, where y_T and y_B are rapidities of target and beam nuclei. For comparison the analogous data from the experiment studying forward production in CC collisions at lower energy 1.05 GeV/nucleon [11] are also added.

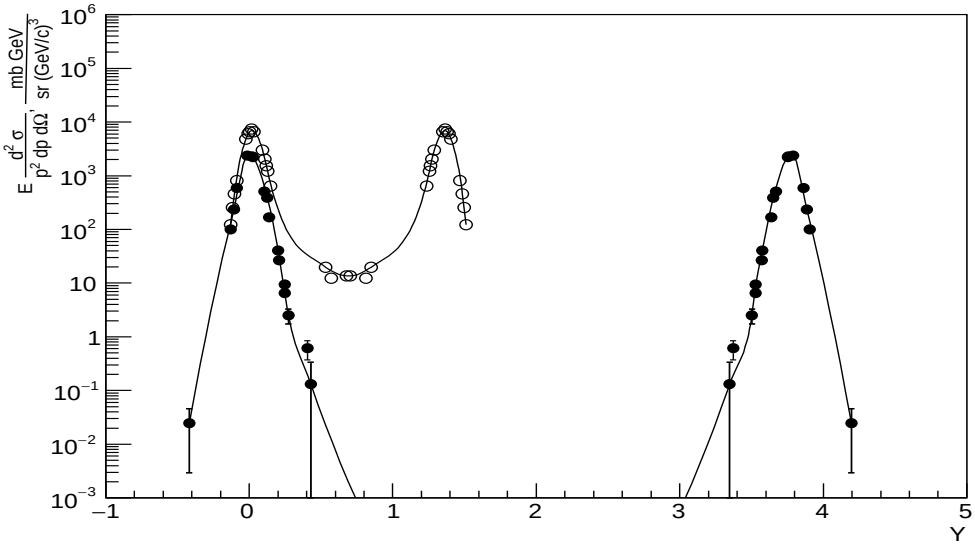

Figure 6. Inclusive differential cross section versus fragment rapidity y in laboratory system for zero angle production of t and ^3He (the data in the target fragmentation region are obtained after the reflection about the point $(y_T + y_B)/2$, where y_T and y_B are rapidities of target and beam nuclei), the black points (•) present data of this experiment, and the open symbols (◦) are given for comparison with analogous measurements in forward direction in CC collisions at lower energy 1.05 GeV/nucleon [11]. The smooth curves are drawn to guide the eye.

The total cross section of nuclear fragmentation σ_f can be approximately estimated as the difference $\sigma_f = \sigma_t - 4\pi R^2$, where σ_t is total cross section and R is radius of carbon nucleus. From the last expression one obtains $\sigma_f = 200$ mb for this experiment. It should be noted that in the talk [1] $\sigma_f = 260$ mb was found by analyzing the available experimental data at low energy band 1-3 GeV/nucleon. The contribution of electromagnetic dissociation σ_e is small in the given experiment. It was calculated as $\sigma_e = 7$ mb in framework of the RELDIS model [36], which describes the fragmentation of nuclei in equivalent photons flux.

4.2. Projectile frame

Figure 7 demonstrates the dependence of Lorentz invariant inclusive differential cross sections in forward direction on fragment momentum in the projectile frame in CC-interactions at energy 20.5 GeV/nucleon (some fragments are omitted in order the picture to be not too cluttered). The statistical model introduced into relativistic nuclear physics by A. Goldhaber [37] gives a simple explanation of the fragmentation processes. It links the observed momentum distribution in the projectile frame with Fermi motion. As a result the form of distribution should be described by Gauss function of the argument A, where A is the atomic number of the observed fragment. In this case the dispersion σ of the distribution obeys the so-called parabolic law

$$\sigma^2 = \sigma_0^2 \cdot A \cdot (A_b - A)/(A_b - 1) \ , \tag{4}$$

where A_b is atomic number of beam nuclei, and σ_0 is expressed through the Fermi momentum P_f as follows:

$$\sigma_0 = P_f/\sqrt{5} \ . \tag{5}$$

The value $\sigma_0 = 96.5$ MeV for ^{12}C was estimated in paper [38] on the basis of phenomenological dependence P_f on A from [39]. It is seen that the invariant cross sections in Figure 7 are not generally described by Gauss function due to the significant differences at large momenta. Therefore, in this work, the fits of distributions presented in Figure 7 are limited to the regions near their maxima. Note that when defined in this way the value of width σ has additional error due to ambiguities in a selection of interval boundaries for the fit.

The found fitted parameter σ characterizing the width of distribution is presented in Figure 8 as a function of atomic number A of the observed nuclear fragment. The solid line is the dependence of σ on A according to the parabolic law (4) with the fixed value $\sigma_0 = 96.5$ MeV. For comparison in this figure the similar analysis are added from article [10] obtained by studying the carbon fragmentation in forward direction in CC-interactions at beam energy 2.1 GeV/nucleon. It can be concluded that the presented data are consistent with the results at lower energies. Generally the experimental dependence of $\sigma(A)$ does not contradict the main predictions of the statistical model taking into account the existing measurement errors.

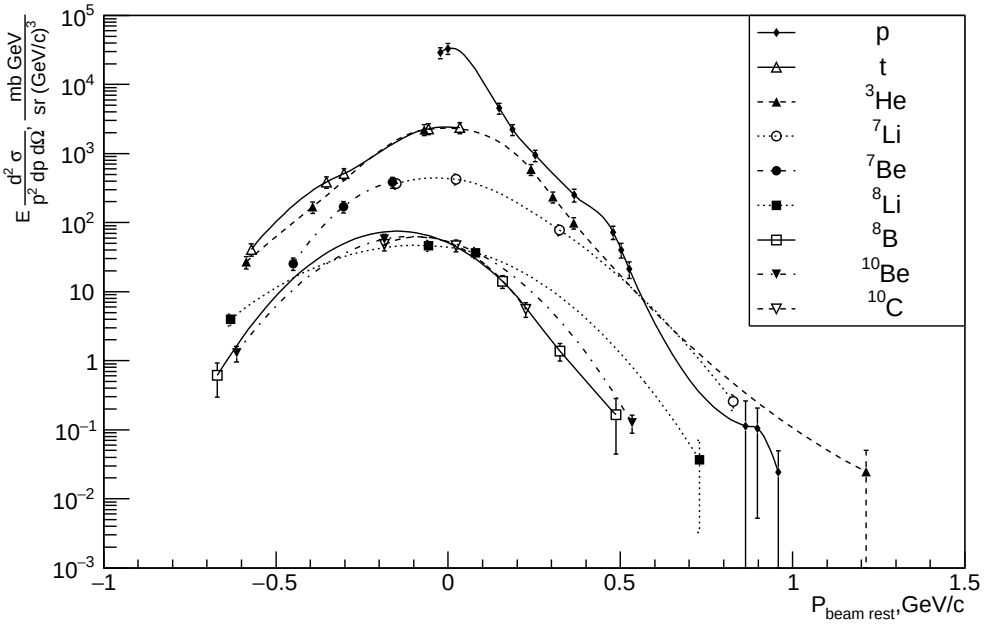

Figure 7. Lorentz invariant inclusive differential cross section for forward production of the fragments versus their momentum in the projectile frame in CC-interactions at energy 20.5 GeV/nucleon. The smooth curves are splines connecting the experimental points.

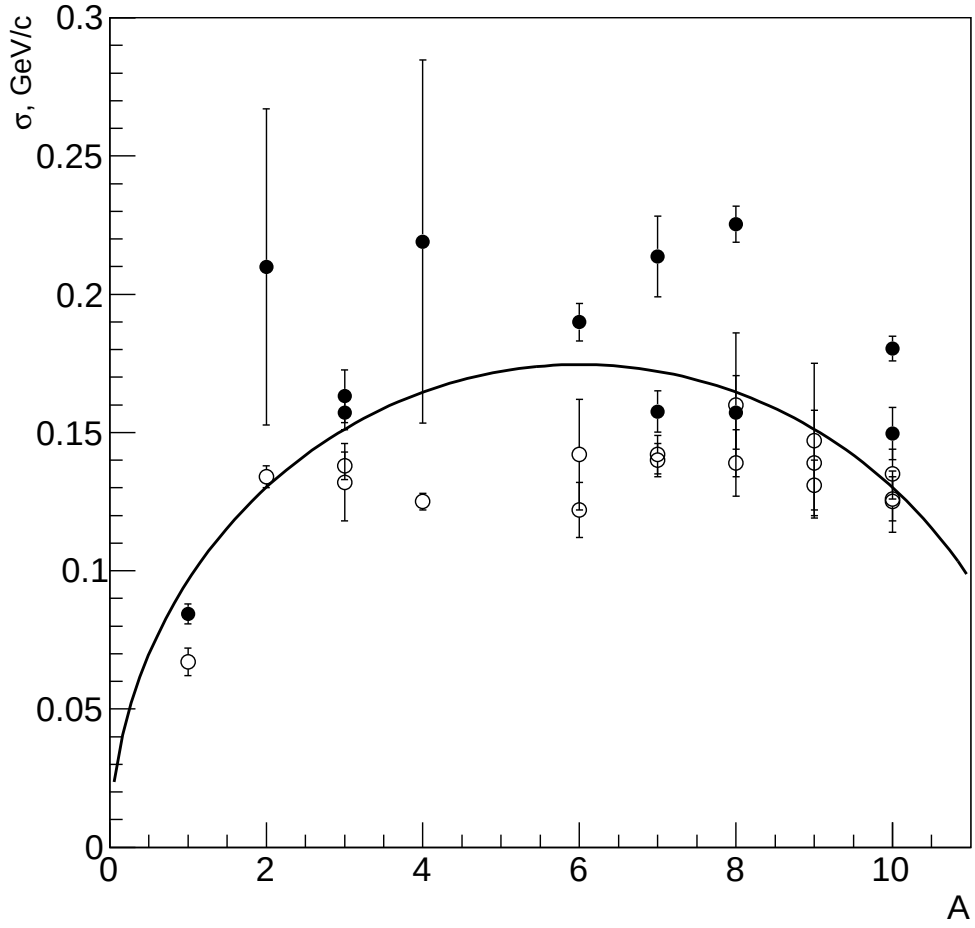

Figure 8. Estimates of the parameter σ characterizing the width (in a vicinity of the maximum) of distributions presented in Figure 7 as a function of atomic number A of the observed nuclear fragment (•), for comparison the similar data [10] of carbon fragmentation in forward direction in CC-interactions at beam energy 2.1 GeV/nucleon are added (∘). The solid line is the dependence of σ on A according to the parabolic law (4) with the fixed value $\sigma_0 = 96.5$ MeV.

Conclusions

Inclusive differential cross sections for the forward production of nuclei are measured in CC-interactions depending on their momentum at beam energy 20.5 GeV/nucleon ($\sqrt{S_{NN}}$ =6.3 GeV). The data show that the maxima of distributions are shifted towards large momenta proportionally to the fragment atomic number A. All fragments are substantially produced in the region beyond the observed peaks with momenta $P_{lab} > A \cdot p_0$, where p_0 is momentum of one nucleon in the ^{12}C beam, i.e. in the kinematical forbidden region in free NN collisions.

The comparison of these data with analogous results at lower energy 1.05 GeV/nucleon shows that the general dependence of cross sections on the variable x=P_{lab}/p_0 is similar, but they are noticeably lower at larger energy 20.5 GeV/nucleon. The mentioned difference varied from a factor of 5 times near the fragmentation peak to several orders of magnitude beyond this peak.

The t/p ratio for the invariant differential cross sections of light nuclei from the peaks of distributions is not essential changed from $\simeq 3.5 \cdot 10^{-2}$ at energy 1.05 GeV/nucleon to $\simeq 4.5 \cdot 10^{-2}$ at 20.5 GeV/nucleon. While in the STAR experiment much smaller value of the similar $t/p \simeq 5 \cdot 10^{-4}$ was measured for integrated fragment yields in central Au-Au collisions at $\sqrt{S_{NN}}$=7.7 GeV. This demonstrates a strong difference of the t/p ratio for fragmentation processes and central collisions.

The measurements were compared to such models like the FTFP (Fritiof) integrated in Geant4 and Goldhaber's statistical model. These models qualitatively describe the main features of cross sections behavior but nevertheless quantitatively there are noticeable discrepancies.

The value of energy considered in this experiment is the highest one for experiments with ion beams on a fixed target for forward production of nuclear fragments with rapidities exceeding the rapidity of projectile particle.

This work was supported by the grant from the Russian Foundation for Basic Research № 19-02-00278.

Table 1. Dependence of the Lorentz invariant inclusive differential cross section $Ed^2\sigma/(p^2dpd\Omega)$ [mb/(GeV$^2c^{-3}$sr)] on momentum P_{lab} in laboratory system in CC-interactions at beam energy 20.5 GeV/nucleon for forward production of nuclear fragments with charge Z=1: proton (p), deuteron (d), tritium (t) (only statistical errors are indicated).

P_{lab}, GeV/c	p	d	t
20.00	2.88e+04 ± 1.47e+02		
20.50	3.32e+04 ± 1.17e+02		
24.00	4.55e+03 ± 2.80e+01		
25.00	2.23e+03 ± 1.59e+01	2.44e+01 ± 2.10e+00	
26.75	9.44e+02 ± 1.24e+01	5.22e+01 ± 3.45e+00	
30.00	2.51e+02 ± 8.65e+00	1.20e+02 ± 6.99e+00	
33.50	7.22e+01 ± 2.97e+00	3.57e+02 ± 7.68e+00	
34.25	4.03e+01 ± 2.51e+00	3.81e+02 ± 9.47e+00	
35.00	2.13e+01 ± 2.08e+00	3.85e+02 ± 1.08e+01	
46.75	1.13e-01 ± 1.28e-01	4.61e+02 ± 7.22e+00	2.51e+00 ± 7.77e-01
48.00	1.05e-01 ± 8.12e-02	3.38e+02 ± 4.25e+00	6.53e+00 ± 8.04e-01
50.25	2.42e-02 ± 2.10e-02	1.96e+02 ± 1.98e+00	4.08e+01 ± 9.78e-01
54.25		2.70e+01 ± 6.32e-01	3.85e+02 ± 2.43e+00
55.25		1.54e+01 ± 5.19e-01	5.11e+02 ± 3.03e+00
60.25		2.61e+00 ± 3.69e-01	2.29e+03 ± 1.10e+01
62.25		1.29e+00 ± 1.57e-01	2.37e+03 ± 6.53e+00

Table 2. Same as Table 1 but for the nuclear fragments with Z=2: ^{3}He, ^{4}He, ^{6}He.

P_{lab}, GeV/c	^{3}He	^{4}He	^{6}He
40.00	1.31e-01 ± 2.08e-01		
41.00	6.10e-01 ± 2.37e-01		
48.00	9.50e+00 ± 6.38e-01		
50.00	2.68e+01 ± 7.83e-01		
53.50	1.68e+02 ± 2.23e+00		
60.00	2.21e+03 ± 1.06e+01		
67.00	5.88e+02 ± 3.28e+00	8.95e+00 ± 4.34e-01	
68.50	2.34e+02 ± 2.03e+00	1.98e+01 ± 6.62e-01	
70.00	9.93e+01 ± 1.43e+00	4.02e+01 ± 1.02e+00	
93.50	2.45e-02 ± 2.16e-02	2.13e+01 ± 4.60e-01	
96.00		3.38e+00 ± 1.53e-01	
100.50		5.44e-01 ± 3.50e-02	4.60e-02 ± 1.15e-02
108.50		9.72e-03 ± 3.00e-03	2.74e-01 ± 2.41e-02
110.50		6.24e-03 ± 2.87e-03	4.12e-01 ± 3.53e-02
120.50			2.06e+01 ± 4.04e-01
124.50			3.47e+01 ± 2.91e-01
140.50			3.15e-01 ± 1.68e-02

Table 3. Same as Table 1 but for the nuclear fragments with Z=3: ^{7}Li, ^{8}Li, ^{9}Li.

P_{lab}, GeV/c	^{7}Li	^{8}Li	^{9}Li
140.25	3.68e+02 ± 1.93e+00		
144.00	4.26e+02 ± 1.64e+00		
150.75	7.80e+01 ± 3.94e-01	3.95e+00 ± 9.42e-02	
162.75	2.55e-01 ± 1.99e-02	4.64e+01 ± 2.96e-01	
165.75		3.67e+01 ± 2.79e-01	
180.75		3.67e-02 ± 2.71e-02	2.97e+00 ± 1.54e-01
186.75			7.40e+00 ± 1.31e-01

Table 4. Same as Table 1 but for the nuclear fragments with Z=4: ^{7}Be, ^{9}Be, ^{10}Be.

P_{lab}, GeV/c	^{7}Be	^{9}Be	^{10}Be
134.00	2.53e+01 ± 7.12e-01		
137.00	1.69e+02 ± 1.73e+00		
140.00	3.84e+02 ± 2.73e+00		
187.00		1.16e+02 ± 1.00e+00	
192.00		5.45e+00 ± 1.81e-01	1.29e+00 ± 1.02e-01
201.00			5.74e+01 ± 3.81e-01
217.00			1.26e-01 ± 1.54e-02

Table 5. Same as Table 1 but for the nuclear fragments with Z=5 and Z=6: ^{8}B, ^{10}C.

P_{lab}, GeV/c	^{8}B	^{10}C
150.00	6.11e-01 ± 2.07e-01	
167.50	1.41e+01 ± 4.56e-01	
171.25	1.38e+00 ± 1.54e-01	
175.00	1.64e-01 ± 9.06e-02	
201.00		4.82e+01 ± 1.03e+00
205.50		4.66e+01 ± 9.44e-01
210.00		5.56e+00 ± 3.34e-01

References

[1] A.M. Zaitsev, Program of the experiments with light nuclei on the U-70, Scientific session-conference of the nuclear physics section of the Physical Sciences Division of the Russian Academy of Sciences "Physics of fundamental interactions", Institute for High Energy Physics, Protvino, December 22-25, 2008. http://exwww.ihep.su/NSC-08/program.shtml#1
http://www.myshared.ru/slide/375315/

[2] S. Ivanov, on behalf of the U-70 staff, Accelerator Complex U-70 of IHEP: Present Status and Recent Upgrades, Proceedings of RuPAC-2010, Protvino, Russia, 2010. https://accelconf.web.cern.ch/accelconf/r10/papers/tuchz01.pdf

[3] S. Ivanov, on behalf of the U-70 staff, Accelerator Complex U70 of IHEP: Status and Upgrades, Proceedings of RuPAC2014, Obninsk, Kaluga Region, Russia, 2014. http://accelconf.web.cern.ch/accelconf/rupac2014/papers/tux02.pdf

[4] Sergey Ivanov, Accelerator Complex U-70 of IHEP-Protvino: Status and Prospects for Upgrade, Conference Proceedings: C13-08-22, p.170-174 (2015). DOI: 10.1142/9789814663618_003
http://inspirehep.net/record/1375738?ln=ru

[5] M.Yu. Bogolyubsky, A.Yu. Bordanovsky, A.A. Volkov, D.K Elumakhov, V.P. Efremov, A.Yu. Kalinin, A.N. Krinitsyn, V.I. Kryshkin, N.V. Kulagin, V.V. Skvortsov, V.V. Talov, L.K. Turchanovich, The production of particles in forward direction at interactions of protons and nuclei with nuclei (proposal of experiment), Preprint IHEP 2013-11, Protvino, 2013.
http://web.ihep.su/library/pubs/prep2013/ps/2013-11.pdf

[6] A.G. Afonin, N.A. Galyaev, V.N. Gres, Yu.P. Davidenko, V.I. Dianov, A. S. Dyshkant, V.N. Zapolsky, V.I. Kotov, V.P. Kryuchkov, S.N. Lapitsky, V.N. Lebedev, A.V. Maximov, A.V. Minchenko, A.N. Mojbenko, V.S. Seleznev, R.M. Sulyaev, V.I. Terehov, M.A. Holodenko, S.A. Chernyi, Yu.A. Chesnokov, Preprint IHEP 90-38, Protvino, 1990.

[7] V.V. Abramov, B.Yu. Baldin, A.F. Buzulutskov, A.A. Volkov, V.Yu. Glebov, P.I. Goncharov, A.N. Gurjiev, A.S. Dyshkant, V.N. Evdokimov, A.O. Efimov, Yu.P. Korneev, A.N. Krinitsyn, V.I. Kryshkin, M.I. Mutafian, V.M. Podstavkov, A.I. Ronjin, R.M. Sulyaev, L.K. Turchanovich, Instrum. Exp. Tech. 35 (1992) 1006.

[8] M.Yu. Bogolyubsky, Instrum. Exp. Tech. 57 (2014) 519. DOI: 10.1134/S0020441214050030

[9] A.M. Baldin, S.B. Gerasimov, N. Giordensku, V.I. Zubarev, L.L. Ivanova, A.D. Kirillov, V.A. Kuznetsov, N.S. Moroz, V.B. Radomanov, V.N. Ramjin, V.S. Stavinskiy, M.I. Iatsuta, Journal of Nuclear Physics (Phys. of Atom. Nucl., Yadernaya Fizika) 18, №1 (1973) 79.

[10] D.E. Greiner, P.J. Lindstrom, H.H. Heckman, Bruce Cork, F.S. Bieser, Phys. Rev. Lett. 15, №3 (1975) 152.

[11] L. Anderson, W. Bruckner, E.Moeller, S. Nagamiya, S. Nissen-Meyer, L. Schroeder, G. Shapiro, H. Steiner, Phys. Rev. C28, №3 (1983) 1224.

[12] E. Moeller, L. Anderson, W. Bruckner, S. Nagamiya, S. Nissen-Meyer, L. Schroeder, G. Shapiro, H. Steiner, Phys. Rev. C28, №3 (1983) 1246.

[13] B.M. Abramov, P.N. Alekseev, Yu.A. Borodin, S.A. Bulychjov, I.A. Dukhovskoy, A.P. Krutenkova, V.V. Kulikov, M.A. Martemyanov, M.A. Matsyuk, E.N. Turdakina, A.I. Khanov, JETP Lett. 97, №8 (2013) 439. DOI: 10.1134/S002136401308002X

[14] B.M. Abramov, P.N. Alekseev, Yu.A. Borodin, S.A. Bulychev, A.A. Duhovskoy, A.P.Krutenkova, V.V. Kulikov, M.A. Martemianov, M.A. Matsyuk, E.N. Turdakina, A.I. Hanov, Phys. of Atom. Nucl. 78, №3 (2015) 373. DOI: 10.1134/S1063778815020039

[15] B.M. Abramov, P.N. Alekseev, Yu. A. Borodin, S.A. Bulychev, A.A. Duhovskoy, A.P.Krutenkova, V.V. Kulikov, M.A. Martemianov, M.A. Matsyuk, S.G. Mashnik, E.N. Turdakina, A.I. Hanov, Phys. of Atom. Nuclei 79, №5 (2016) 700. DOI: 10.1134/S1063778816050033

[16] B.M. Abramov, P.N. Alekseev, Yu. A. Borodin, S.A. Bulychev, K.K. Gudima, A.A. Duhovskoy, A.P.Krutenkova, V.V. Kulikov, M.A. Martemianov, M.A. Matsyuk, E.N. Turdakina, A.I. Hanov, Phys. of Atom. Nucl. 81 №3 (2018) 330. DOI: 10.1134/S106377881803002X

[17] G. Ambrosini, R. Arsenesku, C. Baglin, J. Beringer, C. Bohm, K.Borer, A. Bussiere, K. Elsener, Ph. Gorodetzky, J.P. Guillaud, S. Kabana, R. Klingenberg, G. Lehmann, T.Linden, K.D. Lohmann, R. Mommsent, U. Moser, K. Pretzl, J.Schacher, R. Spiwoks, J. Tuominiemi, M. Weber, New Journal of Physics 1 (1999) 23.1-23.18.

[18] R. Arsenesku, C. Baglin, H.P. Beck, K. Borer, A. Bussiere, F. Dittus, K. Elsener, Ph. Gorodetzky, J.P. Guillaud, P. Hess, S. Kabana, R. Klingenberg, T.Linden, K.D. Lohmann, R. Mommsent, U. Moser, K. Pretzl, J.Schacher, B. Selden, F. Stoffel, J. Tuominiemi, M. Weber, Q.P. Zhang, New Journal of Physics 5 (2003) 150.1-150.23.

[19] M.Yu. Bogolyubsky, A.Yu. Bordanovsky, A.A. Volkov, D.K Elumakhov, V.P. Efremov, A.Yu. Kalinin, A.N. Krinitsyn, V.I. Kryshkin, N.V. Kulagin, V.V. Skvortsov, V.V. Talov, L.K. Turchanovich, Phys. of Atom. Nucl. 80, №3 (2017) 455. DOI: 10.1134./S1063778817020090

[20] M.Yu. Bogolyubsky, A.Yu. Bordanovsky, A.A. Volkov, D.K Elumakhov, V.P. Efremov, A.Yu. Kalinin, A.N. Krinitsyn, V.I. Kryshkin, N.V. Kulagin, V.V. Skvortsov, V.V. Talov, L.K. Turchanovich, Journal of Physics: Conference Series -

http://iopscience.iop.org/issue/1742-6596/934/1. KnowledgeE Publishing Platform - https://knepublishing.com/index.php/KnE-Energy/issue/view/84, The 3rd International Conference on Particle Physics and Astrophysics (ICPPA), 2–5 October 2017, Moscow, Russia (2018) 97, ISSN: 2413-5453. DOI: 10.18502/ken.v3i1.1729

[21] A.G. Afonin, V.N. Gres, V.I. Terekhov. Particle accelerator: Proceedings, 6th European conference, EPAC 98, Stockholm, Sweden, June 22-26, 1998, pp. 1613-1614.

[22] M.Yu. Bogolyubsky, A.A. Volkov, D.K. Elumakhov, A.A. Ivanilov, A.Yu. Kalinin, A.N. Krinitsyn, V.I. Kryshkin, N.V. Kulagin, D.I. Patalakha, K.A. Romanishin, V.V. Skvortsov, V.V. Talov, L.K. Turchanovich, Instrum. Exp. Tech. 62, №5 (2019) 615. DOI: 10.1134/S0020441219050051

[23] V.V. Abramov, A.V. Alekseev, B.Yu. Baldin, V.G. Vasil'chenko, A.A. Volkov, Yu.N. Vrazhnov, A.O. Efimov, Yu.P. Korneev, V.I. Kryshkin, V.E. Rakhmatov, A.I. Ronzhin, V.I. Rykalin and R.M. Sulyaev, Nucl. Instr. Meth. A235 (1985) 497.

[24] A A. Volkov, A.Yu. Kalinin, A.V. Korablev, A.N. Krinitsyn, V.I. Kryshkin, V.V. Skvortsov, V.V. Talov, L.K. Turchanovich, Instrum. Exp. Tech. 53, №4 (2010) 500. https://link.springer.com/article/10.1134/S0020441210040056

[25] http://geant4.cern.ch/support/ReleaseNotes4.10.2.html

[26] M.Yu. Bogolyubsky, D.K Elumakhov, A.I. Ivanilov, A.N. Krinitsyn, Instrum. Exp. Tech. 62, №6 (2019) 5. DOI: 10.1134/S0020441219050130

[27] http://geant4.cern.ch/support/proc_mod_catalog/models/hadronic/FTFP.html

[28] V. Uzhinsky, Joint internatiobnal conference on supercomputing in nuclear application and Monte-Carlo 2010 (SNA-MC2010 Hitotsubashi Hall), Tokio, Japan, October 17-21, 2010. https://geant4.web.cern.ch/sites/geant4.web.cern.ch/files/geant4/results/papers/Fritiof-MC2010.pdf

[29] V.M. Golovin, I.A. Golutvin, S.N. Dolia, B.E. Zhilcov, A.V. Zarubin, V.V. Perelygin, V.S. Sviridov, V.V. Tikhomirov, V.I. Tsovbun, A.G. Fedunov, JINR Rapid Communication № 17-86, Dubna, 1986.

[30] A.A. Baldin, Phys. of Atom. Nucl. 56, №3 (1993) 385.

[31] A.M. Baldin, Bulletin of the Levedev Phisics Institute №1 (1971) 5, Moscow.

[32] Yu.D. Bayukov, L.S. Vorobiev, G.A. Leksin, V. L. Stolin, V.B. Fedorov, V.D. Khovansky, Jounal of Nuclear Physics (Phys. of Atom. Nucl., Yadernaya Fizika) 18, №6 (1973) 1246.

[33] V.S. Stavinskii, JINR Rapid Communications № 18-56, Dubna (1986).

[34] V. K. Bondarev, Physics of Particles and Nuclei 28, №1 (1997) 13.

[35] Hui Liu, Dingway Zhang, Shu He, Ning Yu, Xiaofeng Luo, arHiv:1909.09304v1 [nucl-th] 20 Sep 2019.

[36] I.A. Phenichnov, Physics of Particles and Nuclei 42, №2 (2011) 215.

[37] A.S. Goldhaber, Phys. Lett. B53, №4 (1974) 306.

[38] B.M. Abramov, P.N. Alexeev, Yu. A. Borodin, S.A. Bylychjov, I.A. Dukhovskoy, A.I. Khanov, A.P. Krutenkova, V.V. Kulikov, M.A. Martemianov, M.A. Matsyuk, E.N. Turdakina, Journal of Physics - Conference Series 798(1):012077 (2017). DOI: 10.1088/1742-6596/798/1/012077

[39] M. Giacomelli, L. Sihver, J. Skvarc, N. Yasuda, R. Ilie, Phys. Rev. C69 064601 (2004).

Received August 22, 2019.

Препринт отпечатан с оригинала-макета, подготовленного авторами.

Афонин А.Г. и др.
Рождение вперед ядерных фрагментов в углерод-углеродных столкновениях при энергии пучка 20.5 ГэВ/нуклон.

Оригинал-макет подготовлен с помощью системы **LaTeX.**

Подписано к печати 06.09.2019. Формат 60 × 84/16. Цифровая печать.
Печ.л. 1.25. Уч.-изд.л. 2.02. Тираж 80. Заказ 9. Индекс 3649.

НИЦ «Курчатовский институт» – ИФВЭ
142281, Московская область, г. Протвино, пл. Науки, 1

www.ihep.ru; библиотека http://web.ihep.su/library/pubs/all-w.htm

Индекс 3649

П Р Е П Р И Н Т 2019–6,
НИЦ «Курчатовский институт» – ИФВЭ, 2019